



UNIVERSITY OF LEEDS

This is a repository copy of *Mid-infrared detection in p-GaAs/AlGaAs heterostructures with a current blocking barrier*.

White Rose Research Online URL for this paper:
<http://eprints.whiterose.ac.uk/114565/>

Version: Accepted Version

Proceedings Paper:

Chauhan, D, Perera, AGU, Li, L et al. (2 more authors) (2017) Mid-infrared detection in p-GaAs/AlGaAs heterostructures with a current blocking barrier. In: Proceedings of SPIE. Fourth Conference on Sensors, MEMS, and Electro-Optic Systems, 18-20 Sep 2016 Society of Photo-optical Instrumentation Engineers (SPIE) . ISBN 9781510605138

<https://doi.org/10.1117/12.2242898>

© 2017, Society of Photo Optical Instrumentation Engineers (SPIE). This is an author produced version of a paper published in Proceedings of SPIE. One print or electronic copy may be made for personal use only. Systematic reproduction and distribution, duplication of any material in this publication for a fee or for commercial purposes, or modification of the contents of the publication are prohibited.

Reuse

Unless indicated otherwise, fulltext items are protected by copyright with all rights reserved. The copyright exception in section 29 of the Copyright, Designs and Patents Act 1988 allows the making of a single copy solely for the purpose of non-commercial research or private study within the limits of fair dealing. The publisher or other rights-holder may allow further reproduction and re-use of this version - refer to the White Rose Research Online record for this item. Where records identify the publisher as the copyright holder, users can verify any specific terms of use on the publisher's website.

Takedown

If you consider content in White Rose Research Online to be in breach of UK law, please notify us by emailing eprints@whiterose.ac.uk including the URL of the record and the reason for the withdrawal request.



eprints@whiterose.ac.uk
<https://eprints.whiterose.ac.uk/>

Mid-Infrared detection in p-GaAs/AlGaAs heterostructures with a current blocking barrier

Dilip Chauhan¹, A. G. Unil Perera^{1,*}, Lianhe Li², Li Chen², Edmund H. Linfield²

¹Department of Physics and Astronomy, Georgia State University, Atlanta, Georgia, 30303, USA;

²School of Electronic and Electrical Engineering, University of Leeds, Leeds LS2 9JT, United Kingdom

ABSTRACT

For the infrared detection in the 3-5 μm range, p-GaAs/Al_xGa_{1-x}As heterojunction is an attractive material system due to light hole/heavy hole and spin-orbit split-off intra-valance band transitions in this wavelength range. Varying the Al mole fraction (x) provides the tuning for the wavelength threshold, while graded Al_xGa_{1-x}As potential barriers create an asymmetry to allow a photovoltaic operation. The photovoltaic mode of operation offers the advantage of thermal noise limited performance. In our preliminary work, a 2 – 6 μm photovoltaic detector was studied. Implementation of an additional current blocking barrier improved the specific detectivity (D^*) by two orders of magnitude, to 1.9×10^{11} Jones at 2.7 μm , at 77K. At zero bias, the resistance-area product (R_0A) had a value of $\sim 7.2 \times 10^8 \Omega \text{ cm}^2$, which is five orders higher in magnitude (with a corresponding reduction of the responsivity by only a factor of ~ 1.5), compared to the R_0A value without the blocking barrier. A photoresponse was observed up to 130K.

Keywords: Mid-infrared, current blocking barrier, GaAs/AlGaAs heterostructures.

1. INTRODUCTION

Infrared (IR) detectors and imaging systems are important in diverse areas including military and civilian applications. As the applications in medical imaging and diagnostics, industrial energy loss monitoring, scientific researches such as IR astronomy and global monitoring of environmental pollution and climate change, firefighting, search and rescue, security surveillance, driving, navigation, and numerous other fields increase, demands are growing for low cost, small size and high performance infrared imaging systems. Various types of IR detectors have been studied, including HgCdTe photodiodes,¹ quantum dot IR photodetectors,² quantum well IR photodetectors,³ and type-II superlattice IR photodetectors⁴. In a number of recent works, attention has been paid to the detector structures incorporating current blocking structures into detector designs. AlGaAs current blocking layers were utilized in quantum dot IR photodetectors (QDIPs) to enhance performance.⁴⁻⁸ Similarly, majority carrier (hole) blocking layers have been implemented in type II InAs/GaSb superlattice (T2SL) IR photodetectors.⁹ Furthermore, electron blocking and hole blocking unipolar barriers were implemented in complementary barrier infrared detectors (CBIRD)¹⁰ and p-type-intrinsic-n-type (PbIn) photodiodes¹¹. The most important goal in these architectures is to lower the dark current with a relatively small compromise in the photocurrent. This leads to achieving a significant improvement in the specific detectivity (D^*). Moreover, the mature growth and established processing technology have made p-GaAs/ Al_xGa_{1-x}As materials systems increasingly attractive for heterojunction interfacial workfunction IR photodetectors (HEIWIP),¹² which operate up to room temperature.¹³ In addition, by replacing the constant Al_xGa_{1-x}As barrier with a graded barrier, achieved by varying the Al mole fraction (x), the detector was found capable of operation in photovoltaic mode.¹⁴ This is particularly advantageous over photoconductive operation due to its thermal noise limited performance and reduced power consumption. In this article, we report a 30 period p-GaAs/ Al_xGa_{1-x}As heterojunction IR detector with graded barriers, with an additional current blocking barrier (CBB). This detector shows a photoresponse in the spectral range of $\sim 2-6 \mu\text{m}$, under photovoltaic operation. Approximately five orders of magnitude higher resistance area product (R_0A) at zero bias was observed, resulting in a two orders of magnitude improvement in D^* . The responsivity with the CBB was compromised only by a factor of ~ 1.5 compared to that without the CBB.

*uperera@gsu.edu

2. DEVICE DESIGN AND EXPERIMENTS

A p-GaAs/ $\text{Al}_x\text{Ga}_{1-x}\text{As}$ heterojunction IR detector was grown on a semi-insulating GaAs substrate by molecular beam epitaxy. A schematic of the detector is shown in Figure 1(a). The active region of the detector consists of 30 periods of a 20 nm p-GaAs emitter and 60 nm graded $\text{Al}_x\text{Ga}_{1-x}\text{As}$ barrier layer, sandwiched between highly doped p^+ -GaAs contact layers. All the p-GaAs emitters are doped at $1.0 \times 10^{19} \text{ cm}^{-3}$, whereas all $\text{Al}_x\text{Ga}_{1-x}\text{As}$ barriers are undoped. A 60 nm graded $\text{Al}_x\text{Ga}_{1-x}\text{As}$ CBB layer, followed by another p^+ -GaAs contact layer, were then grown on top of the active region. Thus, there are three p^+ -GaAs contact layers, namely the top, middle and bottom contacts, with the thicknesses of 0.2 μm , 0.5 μm , and 0.7 μm respectively. Measurements between the top and bottom contacts include the CBB, but the middle and bottom contacts measure the same mesa without the CBB. As a result, the same mesa can be studied with the CBB, and without it. The mesas were processed by a combination of conventional photolithography and wet etching, and were

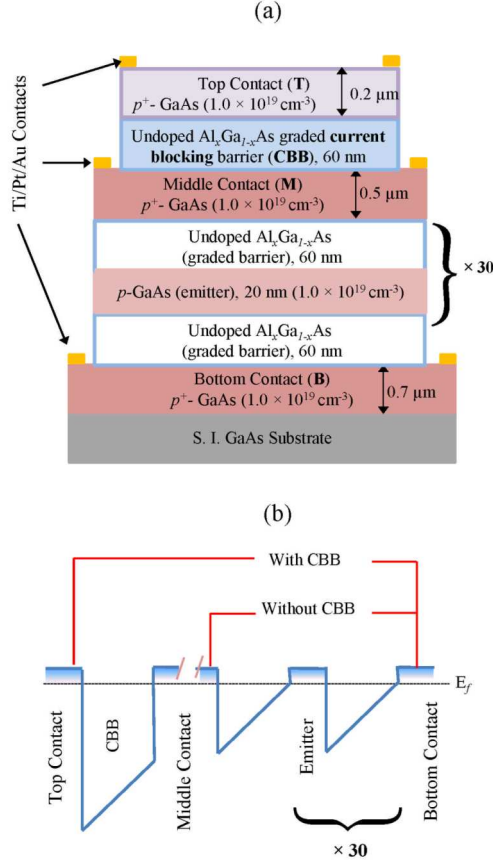


Figure 1. (a) Schematic of the p-GaAs/ $\text{Al}_x\text{Ga}_{1-x}\text{As}$ heterostructure, including the current blocking barrier (CBB). The top and bottom contacts are used to measure with the CBB, and the middle and bottom contacts can be used to measure the same mesa without it. (b) Schematic of the valence band alignment under equilibrium. The $\text{Al}_x\text{Ga}_{1-x}\text{As}$ barriers are graded by tuning the Al mole fraction, x .

followed by Ti/Pt/Au metallization on the top, middle, and bottom contact layers. The areas of the top and middle mesa contacts are $400 \mu\text{m} \times 400 \mu\text{m}$, and $570 \mu\text{m} \times 570 \mu\text{m}$, respectively. Finally, top p^+ -GaAs contact layer was partially etched leaving a $\sim 20 \text{ nm}$ region, to open an optical window of an area $\sim 260 \mu\text{m} \times 260 \mu\text{m}$, (Inset, Figure 2) for a normal incidence optical illumination. The valence band offset between the p-GaAs emitter and the $\text{Al}_x\text{Ga}_{1-x}\text{As}$ barrier leads to an interfacial work function,¹² which is controlled by x in the $\text{Al}_x\text{Ga}_{1-x}\text{As}$ barrier. The energy difference between the Fermi level and the barrier is equal to the minimum energy required for internal photoemission, denoted as the activation energy (Δ). A schematic of the equilibrium valence band alignment of the p-GaAs/ $\text{Al}_x\text{Ga}_{1-x}\text{As}$ heterojunction is depicted in Figure 1(b). The $\text{Al}_x\text{Ga}_{1-x}\text{As}$ barriers are graded, by tuning the x , from $x_1 = 0.03$ at the

bottom to $x_2 = 0.50$ at the top of each barrier. As a result, a potential gradient builds-up across the barrier. The valence band offsets at the p-GaAs/ $\text{Al}_x\text{Ga}_{1-x}\text{As}$ interface, calculated using the temperature-dependent internal photoemission spectroscopy (TDIPS) method¹⁵ are ~ 17 meV, and ~ 280 meV for $x = 0.03$ and $x = 0.50$ respectively, leading to an average potential gradient of ~ 44 kV/cm across each $\text{Al}_x\text{Ga}_{1-x}\text{As}$ barrier. Similarly, the $\text{Al}_x\text{Ga}_{1-x}\text{As}$ CBB was graded by varying x , from $x_1 = 0.53$ at the bottom to $x_2 = 1$ at the top, with the valence band offsets of ~ 290 meV and ~ 550 meV respectively, so that the potential gradient across it is also ~ 44 kV/cm.

In the degenerately p-doped GaAs, the Fermi level lies in the light hole (LH)/heavy hole (HH) band, with the spin-orbit split-off (SO) band separated by ~ 340 meV from the LH/HH band near $k = 0$. For IR detection, light absorption leads to hole transitions from the LH/HH bands to the SO band and from the HH to LH bands, leading to an internal photoemission and escape of the holes over the barriers, which are swept out and collected at the contacts. Free carrier absorption is also possible, resulting in photo-excitation in the HH/LH bands. This process is weaker at shorter wavelengths, but increases with the wavelength¹⁶ as λ^2 . Thus, a p-GaAs layer absorbs a broad IR spectrum. However, the minimum energy required for internal photoemission and escape over the $\text{Al}_x\text{Ga}_{1-x}\text{As}$ barrier is determined by the interfacial work function at the heterojunction. Therefore, the spectral range of the photodetector can be tailored by controlling x . Depending on their energy, the holes can escape to either the S-O band or the H-H/L-H bands in the barrier. A detailed account of possible escape pathways is provided elsewhere,¹⁷ but the asymmetry of the GaAs/ $\text{Al}_x\text{Ga}_{1-x}\text{As}$ barriers plays an important role in driving the holes, even in the absence of an applied bias. Therefore, a net photocurrent can be observed under photovoltaic operation.

The current-voltage measurements were carried out at 77K, using a Keithley 2400 source meter and a Keithley 616 digital electrometer. Positive bias across top-bottom contacts is defined as the voltage connected to the top contact, with the bottom contact grounded. Similarly, in the middle-bottom contacts measurements, voltage is connected to middle contact and the bottom contact is grounded, leaving the top contact open. The spectral responses were measured using a Fourier transform infrared (FTIR) spectrometer, and calibrated by measuring the background by a Si composite bolometer of known sensitivity.

3. RESULTS AND DISCUSSION

The current voltage characteristics at 77K are shown in Figure 2, with bias dependence of the dark current densities being asymmetrical, as a result of the asymmetrical barrier structure. It was found that the CBB lowered the dark current

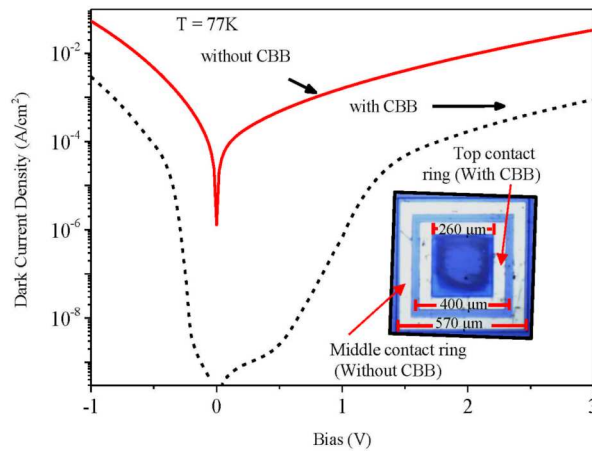


Figure 2. The dark current density of the detector with CBB is five orders of magnitude smaller at low bias, than without the CBB. The difference becomes smaller as the bias increases. Inset: Top view optical image of the detector mesa showing the lateral dimensions of the top contact ($400 \mu\text{m} \times 400 \mu\text{m}$) and middle contact ($570 \mu\text{m} \times 570 \mu\text{m}$), with the optical window ($260 \mu\text{m} \times 260 \mu\text{m}$) at the center.

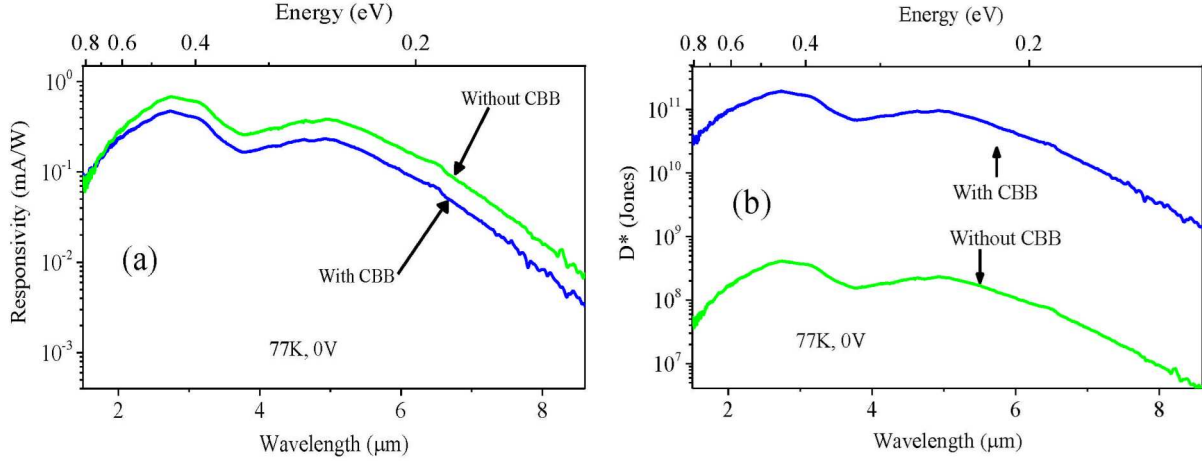


Figure 3. (a) Comparison of the responsivity of the detector showing that the responsivity with the CBB is ~ 1.5 times smaller at zero bias, than without the CBB and without it. (b) Specific detectivity (D^*) under dark conditions, showing a two orders of magnitude higher detectivity with the CBB.

density by five orders of magnitude at low biases, with the difference becoming smaller as the bias increases. The differential resistance-area product (R_0A) at zero bias with the CBB had a value of $\sim 7.2 \times 10^8 \Omega \text{ cm}^2$, compared to a value of $1.6 \times 10^3 \Omega \text{ cm}^2$ obtained without the CBB. The spectral responsivity at zero bias, measured from the same mesa both with and without the CBB, is shown in Figure 3(a). The 340 meV separation of the SO band from the LH/HH band limits the photoresponse from hole transitions between the LH/HH and SO bands to $\sim 3.6 \mu\text{m}$. Beyond $3.6 \mu\text{m}$, there is a photoresponse due to the hole transitions between the HH and LH band. As a result, two distinct response peaks are observed at $2.7 \mu\text{m}$ and $5.0 \mu\text{m}$ with responsivities of 0.67 mA/W and 0.38 mA/W respectively, in the measurements without the CBB. The 50% cut-off levels from these peaks encompass a $\sim 2 - 6 \mu\text{m}$ spectral range. With inclusion of the CBB, the measured responsivity of 0.47 mA/W at $2.7 \mu\text{m}$ is reduced by only a factor of ~ 1.5 from that obtained without the CBB. Specific detectivity (D^*) under dark condition was obtained using:

$$D^* = R_i \sqrt{\frac{R_0A}{4kT}} \quad (1),$$

where R_i (A/W) is the spectral responsivity, k is the Boltzmann constant, k is the temperature, and A (cm^2) is the electrically active area of the detector ($400 \mu\text{m} \times 400 \mu\text{m}$ with the CBB, and $570 \mu\text{m} \times 570 \mu\text{m}$ without the CBB). D^* was found to be $\sim 1.9 \times 10^{11}$ Jones at $2.7 \mu\text{m}$ for the detector with the CBB, and $\sim 4.1 \times 10^8$ Jones without the CBB. Thus, a two orders of magnitude higher D^* is obtained with the CBB at zero bias (Figure 3(b)).

In order to understand effect of the CBB in the spectral range of the detector, we carried out photoresponse measurements in selective spectral ranges, using optical filters with characteristic cut-on wavelengths (λ_{CO}) to block the portion of the incident IR light in the wavelength range shorter than the λ_{CO} as seen the schematic of the IR light path in Figure 4(a). A photoresponse up to $\sim 2.4 \mu\text{m}$ was observed across the top-middle contacts (i.e. across the CBB) without a filter, closely agreeing with $\Delta = 550 \text{ meV}$ for the CBB. This photoresponse disappeared when an optical filter with $\lambda_{\text{CO}} = 2.4 \mu\text{m}$ was introduced on the IR light path (Figure 4(b)). However, when measured between the top-bottom contacts (i.e., with the CBB) with $\lambda_{\text{CO}} = 2.4 \mu\text{m}$ filter being introduced on the IR light path, the photoresponse (corrected for the transmission of the filters) was unaltered in the spectral range longer than λ_{CO} , compared to that without the filter. Also, the photoresponse was unaltered with another optical filter with $\lambda_{\text{CO}} = 4.5 \mu\text{m}$, in the range longer than $4.5 \mu\text{m}$ (Figure 5(a)). Similar results were observed in measurements between middle-bottom contacts (i.e., without the CBB) as seen in the Figure 5(b). The latter case does not include the CBB, therefore the use of the optical filters is not expected to alter

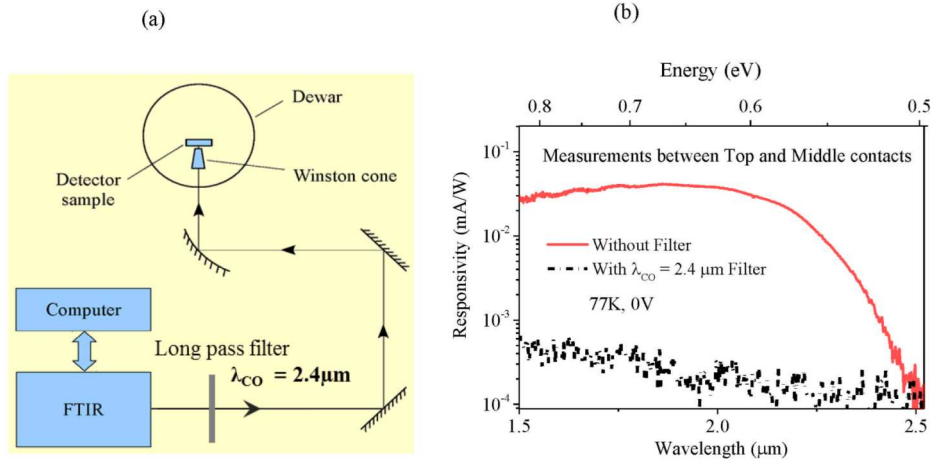


Figure 4. (a) A schematic of the photoresponse measurement set up showing IR light path, where an optical filter of cut-on wavelength λ_{CO} can be introduced to block the IR light in the spectral range shorter than λ_{CO} . (b) The photoresponse measured across top and middle contacts, was disabled by the optical filter with $\lambda_{CO} = 2.4 \mu\text{m}$.

the photoresponse in the spectral range longer than the λ_{CO} . However, in the former case (i.e., with the CBB), disabling the injection of photoexcited holes from the top contact to the middle contact did not affect the photoresponse of the

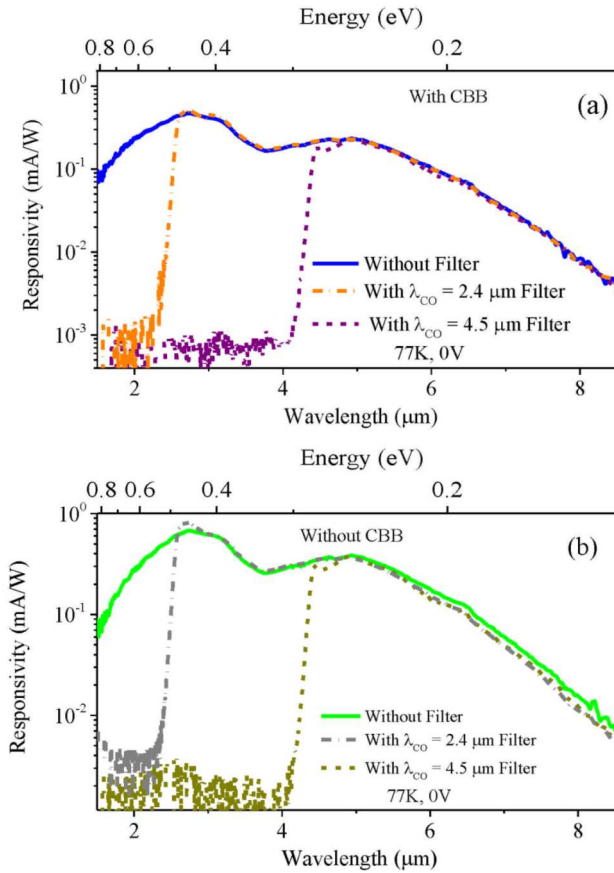


Figure 5. Optical filters of cut-on wavelengths of $\lambda_{CO} = 2.4 \mu\text{m}$ and $4.5 \mu\text{m}$ did not show any effect on the photoresponse in the spectral range longer than λ_{CO} , in the measurements – (a) with the CBB, and (b) without the CBB.

detector with the CBB in the longer than λ_{CO} range. Thus, it was found that the spectral range of the detector is not compromised due to the current blocking barrier.

The photoresponse of the detector was also measured with increasing temperature. A photoresponse was observed up to 130K as seen in Figure 6. Further optimization such as the removal of the thick middle contact layer and instead using a thicker emitter layer may be expected to achieve a higher operating temperature.

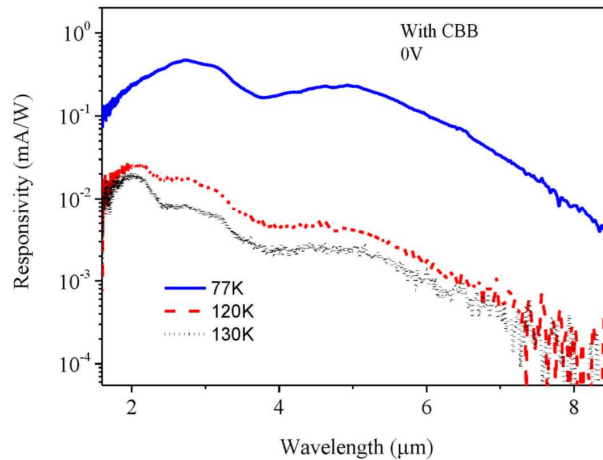


Figure 6. A photoresponse was observed up to 130K at zero bias, in the measurements with the CBB.

4. CONCLUSION

We demonstrated a 30 period p-GaAs/ $Al_xGa_{1-x}As$ heterojunction IR photodetector with a current blocking barrier, showing a photoresponse in mid-infrared spectral range. By incorporating the current blocking barrier, the detectivity was improved by two orders of magnitude. Photovoltaic operation was enabled by graded $Al_xGa_{1-x}As$ barriers, leading to thermal noise limited performance at zero bias. The resistance-area product (R_0A) at zero bias was enhanced by five orders of magnitude due to the current blocking barrier, whereas the responsivity was reduced by only a factor of 1.5. Implementation of current blocking barrier, together with the graded barriers, can be useful for the development of p-GaAs/ $Al_xGa_{1-x}As$ heterojunction detectors.

ACKNOWLEDGMENTS

This work was supported in part by the U.S. Army Research Office under Grant No. W911 NF-15-1-0018, and in part by National Science Foundation (NSF) under Grant No. ECCS-1232184. Funding was also received from the European Community's Seventh Framework Programme (FP7-IDEAS-ERC) under grant agreement number 247375 'TOSCA'. Dilip Chauhan acknowledges GSU Brains & Behavior Fellowship.

REFERENCES

- [1] Martyniuk, P. and Rogalski, A., "HOT Infrared Photodetectors", *Opto-Electron. Rev.* 21 (2), 239 (2013).
- [2] Ariyawansa, G., Perera, A. G. U., Su, X. H., Chakrabarti, S., and Bhattacharya, P., "Multi-color tunneling quantum dot infrared photodetectors operating at room temperature", *Infrared Phys. Technol.* 50 (2-3), 156 (2007).

- [3] Sherliker, B., Halsall, Kasalynas, M., I., Seliuta, D., Wang, T., Buckle, P. D. et al., “Room temperature operation of AlGaIn/GaN quantum well infrared photodetectors at a 3–4 μm wavelength range”, *Semiconductor Science and Technol.* 22 (11), 1240 (2007).
- [4] Hill, C. J., Soibel, A., Ting, D. Z. Y., Keo, S. A., Mumolo, J. M., Nguyen J., Lee, M., and Gunapala, S. D., “High-Temperature Operation of Long-Wavelength Infrared Superlattice Detector with Suppressed Dark Current”, *Electronics Lett.* 45 (21), 1089 (2009).
- [5] Wang, S. Y., Lin, S. D., Wu, H. W., and Lee, C. P., “Low dark current quantum-dot infrared photodetectors with an AlGaAs current blocking layer”, *Appl. Phys. Lett.* 78 (8), 1023 (2001).
- [6] Rotella, P., Raghavan, S., Stintz, A., Fuchs, B., Krishna, S., Morath, C., Le, D., and Kennerly, S. W., “Normal incidence InAs/InGaAs dots-in-well detectors with current blocking AlGaAs layer”, *J. Crystal Growth* 251 (1–4), 787 (2003).
- [7] Wang, S. Y., Lin, S. D., Wu, H. W., and Lee, C. P., “High performance InAs/GaAs quantum dot infrared photodetectors with AlGaAs current blocking layer”, *Infrared Phys. Technol.* 42 (3–5), 473 (2001).
- [8] Lin, S. Y., Tsai, Y. R., and Lee, S. C., “High-performance InAs/GaAs quantum-dot infrared photodetectors with a single-sided $\text{Al}_{0.3}\text{Ga}_{0.7}\text{As}$ blocking layer”, *Appl. Phys. Lett.* 78 (18), 2784 (2001).
- [9] Nguyen, B. M., Bogdanov, S., Pour, S. A., and Razeghi, M., “Minority electron unipolar photodetectors based on type II InAs/GaSb/AlSb superlattices for very long wavelength infrared detection”, *Appl. Phys. Lett.* 95 (18), 183502 (2009).
- [10] Ting, D. Z. Y., Hill, C. J., Soibel, A., Keo, S. A., Mumolo, J. M., Nguyen, J., and Gunapala, S. D., “A high-performance long wavelength superlattice complementary barrier infrared detector”, *Appl. Phys. Lett.* 95 (2), 023508 (2009).
- [11] Gautam, N., Kim, H. S., Kuty, M. N., Plis, E., Dawson, L. R., and Krishna, S., “Performance improvement of longwave infrared photodetector based on type-II InAs/GaSb superlattices using unipolar current blocking layers”, *Appl. Phys. Lett.* 96 (23), 231107 (2010).
- [12] Perera, A. G. U., Matsik, S. G., Yaldiz, B., Liu, H. C., Shen, A., Gao, M., Wasilewski, Z. R., and Buchanan, M., “Heterojunction Wavelength-Tailorable Far-Infrared Photodetectors with Response out to 70 Microns”, *Appl. Phys. Lett.* 78 (15), 2241 (2001).
- [13] Jayaweera, P. V. V., Matsik, S. G., Perera, A. G. U., Liu, H. C., Buchanan, M., and Wasilewski, Z. R., “Uncooled infrared detectors for 3-5 μm and beyond”, *Appl. Phys. Lett.* 93 (2), 021105 (2008).
- [14] Pitigala, P. K. D. D. P., Matsik, S. G., Perera, A. G. U., Khanna, S. P., Li, L. H., Linfield, E. H., Wasilewski, Z. R., Buchanan, M., and Liu, H. C., “Photovoltaic Infrared Detection with p-type Graded Barrier Heterostructures” *J. Appl. Phys.* 111 (8), 084505 (2012).
- [15] Lao, Y. F. and Perera, A. G. U., “Temperature-dependent internal-photoemission probe for band parameters,” *Phys. Rev. B* 86, 195315 (2012).
- [16] Korotkov, A. L., Perera, A. G. U., Shen, W. Z., Herfort, J., Ploog, K. H., Schaff, W. J., and Liu, H. C., “Free-carrier Absorption in Be- and C-doped GaAs Epilayers and Far Infrared Detector Applications”, *J. Appl. Phys.* 89 (6), 3295 (2001).
- [17] Perera, A. G. U., Matsik, S. G., Jayaweera, P. V. V., Tennakone, K., Liu, H. C., Buchanan, M., Winckel, G. V., Stintz, A., and Krishna, S., “High Operating Temperature Split-off Band Infrared Detectors”, *Appl. Phys. Lett.* 89, 131118 (13) (2006).